NUCLEAR
INSTRUMENTS
& METHODS
IN PHYSICS
RESEARCH
Section A

# Shashlik calorimeter Beam-test results

J. Badier <sup>a</sup>, Ph. Busson <sup>a</sup>, C. Charlot <sup>a</sup>, L. Dobrzynski <sup>a,\*</sup>, R. Tanaka <sup>a</sup>, P. Bordalo <sup>b</sup>, S. Ramos <sup>b</sup>, S. Bityukov <sup>c</sup>, V. Obraztsov <sup>c</sup>, A Ostankov <sup>c</sup>, A. Zaitchenko <sup>c</sup>, S. Gninenko <sup>d</sup>, E. Guschin <sup>d</sup>, V. Issakov <sup>d</sup>, Y. Mussienko <sup>d</sup>, I. Semenjuk <sup>d</sup>

Received 3 January 1994; revised form received 28 March 1994

Results from an extensive study of nonprojective Shashlik calorimeter prototypes are reported. Nine  $(47 \times 47 \text{ mm}^2)$  towers were exposed to a high energy electron beam at CERN SPS and read out by silicon photodiodes followed by low noise preamplifiers. The main results are the measurements of the energy and shower position resolution and the angular resolution of the electron shower direction. The shower direction measurement is encouraging being in agreement at the tower center with a resolution of  $\sigma_{\theta}(\text{mrad}) = 70/\sqrt{E}$  (10 mrad for 50 GeV electrons). The uniformity of the calorimeter response is found to be better than  $\pm 1\%$ . The mean light yield measured in Shashlik towers equipped with Kuraray Y7 WLS fibres and aluminized at the front end of the tower is of the order of 13 photons/MeV.

# 1. Introduction

In order to search for new phenomena at the LHC [1] good electromagnetic calorimetry will be essential. Its required performances are currently determined by the decay of the intermediate mass Higgs boson into two photons [2]. The following performance should be achieved:

- energy resolution at least as good as  $\sigma/E = 0.1/\sqrt{E}$  and a constant term of 1%;
- operation in the presence of high magnetic field which could be as large as 4 T;
- high radiation resistance (> 1 Mrad/yr);
- high speed to work with the 25 ns LHC bunch crossing;
- as good a hermeticity as possible.

A Shashlik type calorimeter is designed to meet these requirements. It is a lead/scintillator sandwich calorimeter having the crucial properties of compactness, timing, good spatial resolution and low cost.

In the mid-1980s Fessler et al. [3] suggested the use of WLS optical fibres for the readout of scintillation light from sandwich electromagnetic calorimeters. Four years later INR (Moscow) and IHEP (Protvino) [4] developed a process for mass production of scintillator tiles and lead plates with the holes necessary for the insertion of the WLS fibres. These techniques were used for prototypes

studies for HERA [5] experiments calorimeters and NO-MAD [6]. Beam-test measurement results for a prototype of the calorimeter performed at CERN [6], BNL and IHEP [4] showed that it was possible to obtain good energy resolution and  $\pi/e$  separation, good light collection and light transmission efficiency and promising results with photodetectors operating in high magnetic field (silicon photodiodes, tetrodes, etc.). In addition, these calorimeters showed that the dead space could be minimized thus obtaining good lateral uniformity of response and build a calorimeter with a high degree of hermeticity.

In the context of the CMS [7] (Compact Muon Solenoid) detector, a Shashlik [8] type lead/scintillator calorimeter has become a promising option to fulfill the LHC physics requirements.

#### 2. The Shashlik calorimeter

Each calorimeter module is a lead/scintillator sandwich, made out of perforated lead and plastic scintillator plates. The scintillator plates were manufactured at IHEP with casting technology [9]. This produces plates with a surface of high optical quality including the surface of the holes for fibres. Perforated lead plates, containing 5% antimony additive to increase their rigidity, were manufactured by cold punching. White paper (20 mg/cm, 0.1 mm thick) was placed between the lead and scintillator plates

<sup>&</sup>lt;sup>a</sup> Ecole Polytechnique, IN2P3-CNRS, Palaiseau, France

<sup>&</sup>lt;sup>b</sup> LIP, Lisbon, Portugal

<sup>&</sup>lt;sup>c</sup> IHEP, Protvino, Russian Federation

<sup>&</sup>lt;sup>d</sup> INR, Moscow, Russian Federation

<sup>\*</sup> Corresponding author. E-mail dobj@frcpn11.

Table 1
Main parameters of the CMS prototype Shashlik towers

Tower lateral sizes	47×47 mm <sup>2</sup>
Number of planes	75
Total depth (465 mm)	$27.5X_0$
Mean radiation length $(X_0)$	16.9 mm
Moliere radius	34 mm
Lead thickness	2 mm
Scintillator type	polystyrene + 5% POPOP
	+2% paraterphenyl
Scintillator thickness	4 mm
Type of WLS fibres	<b>Y</b> 7
Number of fibres	25
Fibre diameter	1.2 mm
Hole diameter in scintillator	1.3 mm
Hole diameter in lead	1.5 mm

to act as a reflecting surface. The paper was perforated by the same punch as the lead plates. The module as a whole was wrapped with aluminized Mylar and held together by four bicycle rods fixed to aluminum plates at the front and at the rear of each tower. The parameters of the sampling layers are summarized in Table 1 for the CMS [10] prototype.

The optimal number of WLS fibres in the module was chosen, on the one hand, by the requirement of maximum light collection with minimum lateral nonuniformity (corresponding to a less than 2% contribution to energy resolution) and, on the other hand, by cost and technological considerations. A more precise estimate of the optimal number of fibres was obtained by Monte Carlo calculation of the light collection nonuniformity. The efficiency with which the light is captured by an individual fibre is well described by the model of Labarga and Ros [11].

The WLS fibres are required to have a light attenuation length of at least 1.5 m, when used in 40 cm long Shashlik towers. This limits the effect of the longitudinal fluctuations of the electromagnetic shower to about 1% onto the "constant term" of the energy resolution function. The WLS fibres are required to have good optical uniformity and long-term mechanical stability. The diameter dispersion of the fibres should not exceed  $\pm 0.03$  mm. Non

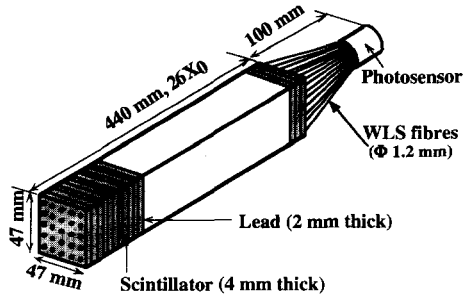


Fig. 1. Mechanical design of a CMS Shashlik calorimeter prototype tower equipped with 25 aluminized WLS fibres.

uniformity in the optical properties of the fibres can lead to a decrease in the light yield and a contribution to the energy resolution of the order  $\sigma/\sqrt{N}$  can be expected ( $\sigma$  is the dispersion of fibre to fibre response and N is the number of fibres which contribute to the total light yield from an electromagnetic shower).

The first WLS fibres used for the Shashlik type prototypes [4–6] were Polychrome-26 fibres developed and produced at INR (Moscow). The core of this optical fibre was made out of polystyrene with a refractive index of n=1.59. The cladding was made out of fluorinated PMMA with n=1.40. The core contains luminophor with the absorption spectrum at  $\lambda_{\rm max}=450$  nm, which matches quite well the emission spectrum of the pterphenyl + POPOP scintillator. The luminophor emission spectrum has  $\lambda_{\rm max}=530$  nm.

The design of an individual CMS prototype module  $(47 \times 47 \times 440 \text{ mm}^3)$  developed by the Ecole Polytechnique–INR–IHEP collaboration is shown in Fig. 1. Table 1 gives its main parameters and characteristics. Each plate of the module has 25 holes in it, arranged as a  $5 \times 5$  square matrix. WLS fibres were inserted into these holes perpendicularly to the plates. The WLS fibres were fed through the entire length of the tower looped around at the front of the tower and fed back through the tower to complete the insertion process. The photomultiplier then sees both ends of the same fibre at once. Such a loop acts

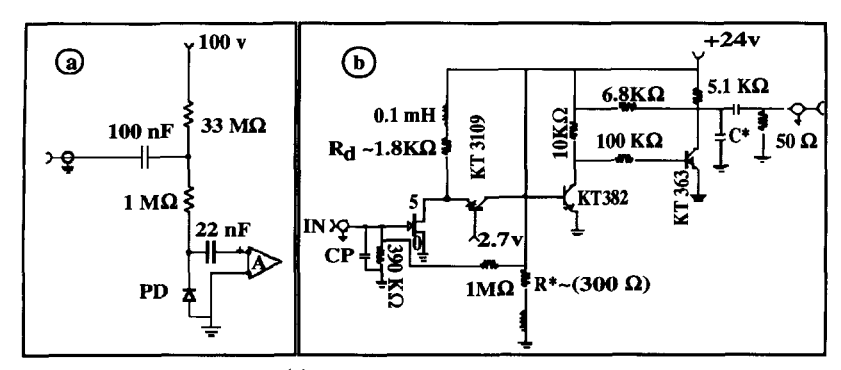


Fig. 2. (a) Power supply of the photodiode; (b) preamplifier design used to read out the CMS prototype Shashlik towers.

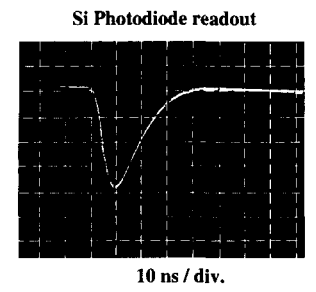


Fig. 3. Observed preamplifier signal output with a detector capacitance of  $C_{\rm D}=30$  pF. The preamplifier is characterized by:  $\tau_{\rm RC-CR}=10$  ns and a gain of 200 mV/10<sup>6</sup> e<sup>-</sup>.

as an almost ideal mirror with a reflection coefficient > 95%. The effective light absorption length in the fibres of the module was  $\sim$  1.2 m. Looping the fibres avoids the necessity of aluminizing the fibres ends at the front of the tower and could lead to a greater uniformity of light collection.

In the CMS modules tested in the beam, we used 13 K27 WLS fibres (12 with loops at the front and one single fibre) and 25 Kuraray Y7 fibres cut at the front of the tower and aluminized [12]. The two methods gave us about the same light yield. The fibres were bunched together at the rear of the tower and cut with a diamond mill. A hexagonal Plexiglas light mixer was used to couple the fibres to a silicon photodiode [13]. Each photodiode ( $C_D$  = 30 pF) was polarized as shown in Fig. 2a and followed by a low noise amplifier (ENC =  $1100 e^{-}$ ) built at INR (Fig. 2b). Fig. 3 gives the observed signal at the preamplifier output. One sees that the peaking time is 10 ns. For the test beam setup, the preamplifiers were connected to a postamplifier by a 50 m long cable increasing such the peaking time to 20 ns. An additional gain adjustable LeCroy amplifier was also used to bring the collected charge within the ADC range [14].

# 3. Test beam setup

The measurements were performed in the H2 beam line of the SPS at CERN. The calorimeter was mounted on a platform which could be moved with a precision better

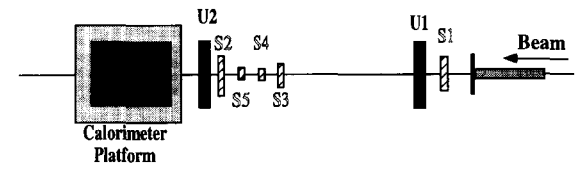


Fig. 4. Test beam layout. The lateral dimensions of  $S_1$  and  $S_2$  are  $10 \times 10$  cm<sup>2</sup>.  $S_3$  is a  $2 \times 2$  cm<sup>2</sup> scintillator.  $S_4$  and  $S_5$  define a  $5 \times 5$  mm<sup>2</sup> beam spot.

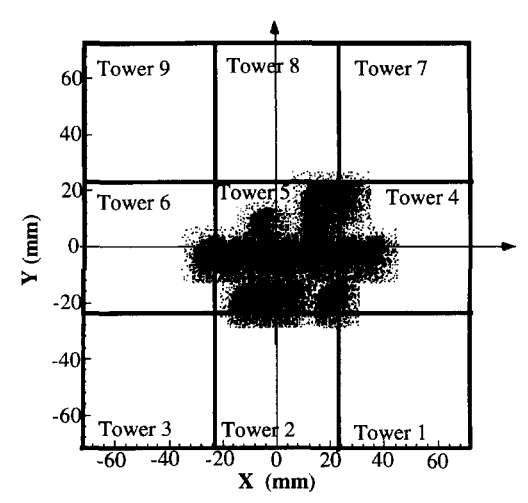


Fig. 5. Shashlik nine tower calorimeter setup. The black points correspond to electron data hitting the calorimeter and used for its uniformity response studies.

than 0.1 mm horizontally and vertically with respect to the beam line. It also allowed the ability to rotate the detector around its vertical axis. Data were taken for electrons hitting the detector at a chosen angle  $\theta_z$  in the horizontal plane, with respect to the fibres axis.

Upstream of the calorimeter, a trigger counter telescope was installed. It consisted of five scintillation counters  $(S_1-S_5)$ . Two MWPC chambers  $(U_1, U_2)$  with x,y readout, situated at 5 m from each other, were used to define the beam impact point into the calorimeter. The beam layout is shown in Fig. 4.

Negative particle beams of 10, 20, 40, 80 and 150 GeV were sent into the detector at  $\theta_z = 0^{\circ}$  with respect to the fibre axis. The beam particle rates were  $10^2-10^3$  events per spill (duration of 2.6 s every 14 s). At high energies ( $\geq$  40 GeV) the beams were very clean, the contamination of  $\pi$  in electron beam was nonexistent. In the analysis we present here, no special treatment was applied to the data to eliminate an eventual pion contamination.

We report here results on a nine tower calorimeter setup assembled in a  $3 \times 3$  matrix as shown in Fig. 5.

# 4. Experimental data and methods

## 4.1. Data taking and triggers

To define a valid electron event hitting the calorimeter we have requested that the  $S_1$ ,  $S_2$  and  $S_3$  counters were in coincidence. This condition defines the wide beam trigger (Trigger 1). The total area covered by the wide beam is  $20 \times 20 \text{ mm}^2$ . When counters  $S_4$  and  $S_5$  were added to the coincidence, defining Trigger 1 condition, we get the so called narrow beam trigger (Trigger 2). The area covered by the narrow beam is  $5 \times 5 \text{ mm}^2$ .

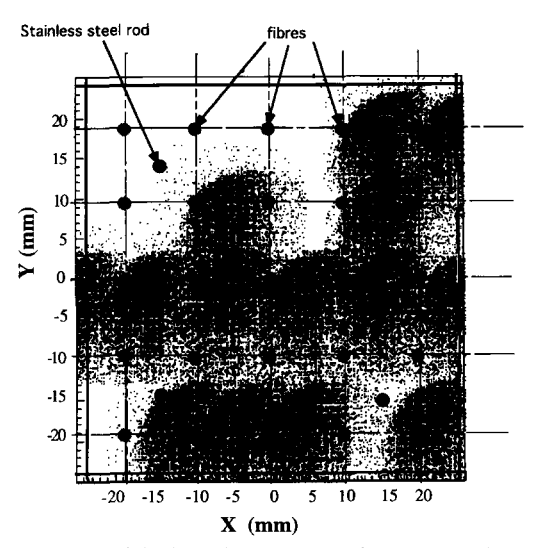


Fig. 6. Recorded 40 GeV electron data hitting tower 5. The black round dots represent the position of the stainless steel rods (4 per tower). The gray round dots represent the position of the fibres (25 per tower).

#### 4.2. Energy calibration of the towers

The towers were calibrated with 40 GeV electrons. About 3000 electrons, taken with Trigger 2 condition, were sent into the central region of each tower (Fig. 5) at normal incidence ( $\theta_z = 0^{\circ}$ ). On average  $\approx 85\%$  of the electromagnetic shower energy is deposited in the tower under calibration. We have adjusted the gain of each LeCroy amplifier to have on-line the same response within few percent for each calorimeter tower. Off-line, the calibration constants were estimated with a statistical precision of 0.2% from these data. For the analysis presented in this paper all measurements were corrected with the calibration constants obtained from off line calibration.

# 4.3. The data

Fig. 6 shows all the taken data. The black round dots are the four stainless steel rods used to fasten the tiles together. The round gray dots are the fibres. The results described in the following sections were obtained by analyzing the following sets of data taken at normal incidence (electron beam parallel to the WLS fibres):

- Electrons of 10, 20, 40, 80 and 150 GeV entering the central region of tower 5 taken with Trigger 2 condition.
   These data were used for the estimation of the energy resolution as well as for the shower position resolution measurement.
- Electrons of 40 GeV hitting tower 5 as shown in Figs. 5 and 6. About 10 000 events have been taken with Trigger 1 condition at different positions in the tower. Starting from the center of the tower data have been taken

every 10 mm in x and y. These data have been used for the study of the uniformity response of the calorimeter. From Fig. 6 one can see that data in the vicinity of the fibres and in all critical parts of the tower (edges, corners) have been accumulated.

- Electrons of 10, 20, 40, 80 and 150 GeV entering the central region of tower 5 preceded by a 2.5 cm thick lead plate were taken with Trigger 2 condition. These data are used to study the ability to reconstruct the shower position in the calorimeter when either a position detector is placed at  $4.5\,X_0$  or a preshower detector is placed at  $3\,X_0$  in front of the calorimeter. The angular resolution of the shower direction presented in this work is obtained from the reconstructed position of the shower in the active part of the calorimeter and the guessed position in a preshower detector.
- Finally we have taken data (Trigger 1) with 225 GeV muons hitting the central region of tower 5.

# 4.4. Selection of the data

The (x, y) coordinates of the electron impact point in the tower are obtained from  $U_1$  and  $U_2$  delay line wire chambers. In order to reduce the noise, we have applied a  $2\sigma$  cut on all x and y beam chamber profiles. In addition, to guarantee the direction of the beam to be parallel to the fibre direction, we have required that the difference in x and y measured by each of these chambers was smaller than 1 mm (0.2 mrad).

#### 4.5. Abnormal calorimeter responses

Fig. 7 shows, for the recorded 40 GeV electrons, the measured energy as function of the X coordinate impact point. In Fig. 8 is given the energy distribution of all the

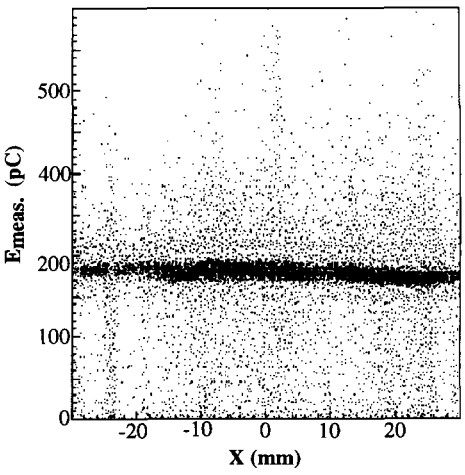


Fig. 7. Event by event measured energy in the Shashlik nonet as function of the X coordinate of the impact point. The 40 GeV electrons are hitting the tower at normal incidence.

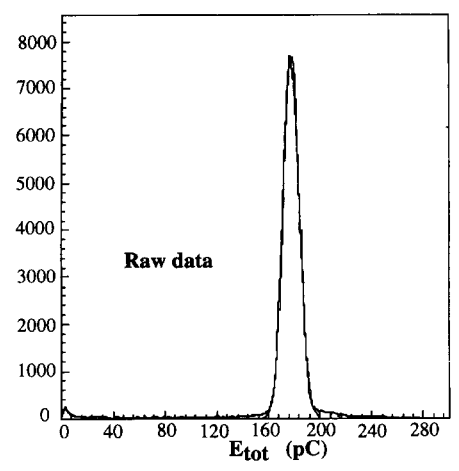


Fig. 8. Measured energy for all the data (131077 events) appearing on Fig. 6. The data which deviate from the Gaussian part of the distribution (3 $\sigma$ ) represent 8% of all events. A Gaussian fit gives:  $E_{\rm mean}=178~{\rm pC}$  and  $\sigma/E=3.49\%$ .

data from Fig. 7. The data which deviate from the Gaussian part of the distribution  $(3\sigma)$  represent 8% of all events. As it will be shown this is mainly due to electron whose incident direction is parallel to the WLS fibres. Fig. 9 gives the X mean profile for all data hitting the calorimeter. The vertical axis is no longer the reconstructed energy as in Fig. 7, but the deviation of the reconstructed energy to the mean fitted energy quoted on Fig. 8. We have indicated on this figure the position of the tower edges as well as the position of the fibres. The minima corresponding to the tower edges are separated by 48 mm. This dimension corresponds to the mechanical dimension of the tower (47 mm) to which is added the thickness of the tower wrapping  $(2 \times 0.5 \text{ mm})$ . The abnormal response due to the tower edges extends over  $\pm 1$  mm. Another source of abnormal response  $(\pm 1 \text{ mm})$  due to channeling in the fibres can be also estimated from Fig. 9. It was checked that, from the Y profile (not shown), the same value for

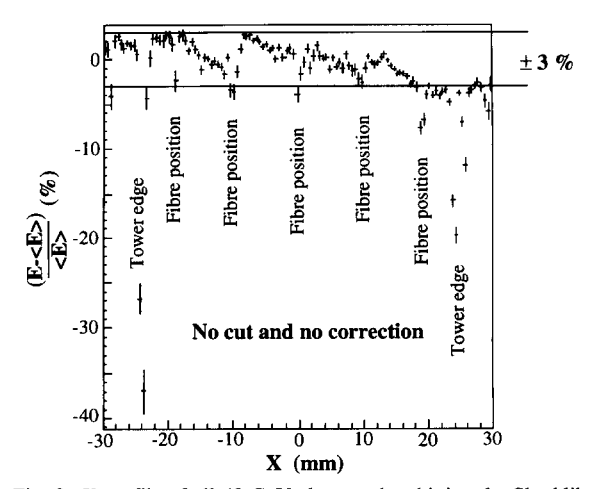
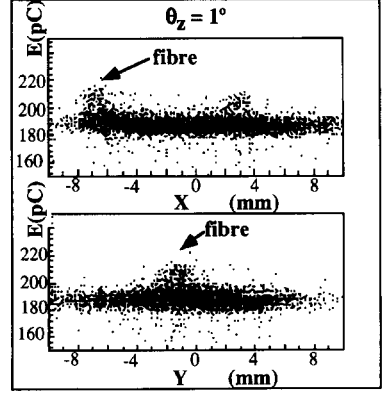


Fig. 9. X profile of all 40 GeV electron data hitting the Shashlik nonet setup. The X bin size is 0.5 mm. Tower edges and fibre positions are indicated.

the tower size, the distance between fibres and abnormal response are observed.

#### 4.6. Correction of abnormal response

The main non-uniformity of response of the Shashlik calorimeter comes from the electrons hitting the fibres and channeling in them (Figs. 7 and 9). To understand this effect, we took data with electrons hitting the calorimeter at an incident angle of  $\theta_z = 1^\circ$  and 3° (Fig. 10). One sees that for  $\theta_z = 1^\circ$  the dispersion of the measured energy in the vicinity of a fibre is still there, but is reduced in comparison with data from a run with  $\theta_z = 0^\circ$  (Fig. 7). The data which deviate from the Gaussian part of the energy distribution (3 $\sigma$ ) represent here 3.7% of the events. A Gaussian fit gives:  $E_{\text{mean}} = 187.2 \text{ pC}$  and  $\sigma/E = 1.81\%$ . The dispersion disappears completely for  $\theta_z = 3^\circ$ . The data which deviate from the Gaussian part of the energy distri-



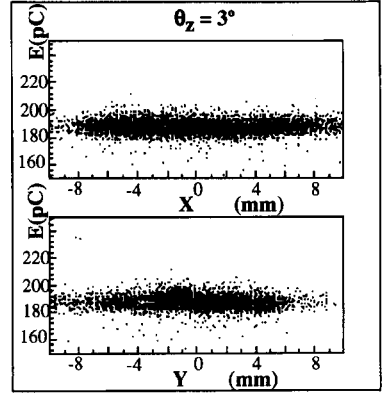


Fig. 10. Calorimeter response for 40 GeV electrons at  $\theta_z = 1^{\circ}$  and  $\theta_z = 3^{\circ}$ .

bution  $(3\sigma)$  represent now only 1.1% of all the events. A Gaussian fit gives:  $E_{\text{mean}} = 187.3 \text{ pC}$  and  $\sigma/E = 1.80\%$ .

Therefore a possible way to correct for the observed abnormal response is to tilt, by a small angle (3° seems to be sufficient) the towers with respect to the incident direction of the particles. In addition, we foresee that a preshower detector placed at  $3X_0$  in front of the calorimeter will also help in reducing this lateral non-uniformity.

## 4.7. Transverse leakage correction of electron showers

The transverse size of the Shashlik nonet is not able to fully contain the energy deposited by an electron of 40 GeV. When the electron hits the center of tower 5, about 2% of the shower energy is leaking the nonet. For the study of the uniformity of the energy response, correction for the energy leaking the setup is mandatory. To estimate this correction, we have studied the variation of the energy for:

- the three right towers (1, 4 and 7) when the beam impact point is running from the center to the left edge of tower 5 (Fig. 5),
- the three left towers (3, 6 and 9) when the beam impact point is running from the center to the right edge of tower 5 (Fig. 5),
- the three top towers (7, 8 and 9) when the beam impact point is running from the center to the down edge of tower 5 (Fig. 5),
- the three down towers (1, 2 and 3) when the beam impact point is running from the center to the top edge of tower 5 (Fig. 5),

We have checked that the energy variation of the left (right) and the top (down) towers have the same dependence. Fig. 11 gives the variations of the leaking energy. Second order polynomials fit well the measured points and will be used to correct the raw data. The result of the correction due to leakage on the raw data is shown in Fig. 12. There still remains an overall linear dependence of the energy when the electron impact point runs over the tower. This variation can be explained by differences in the

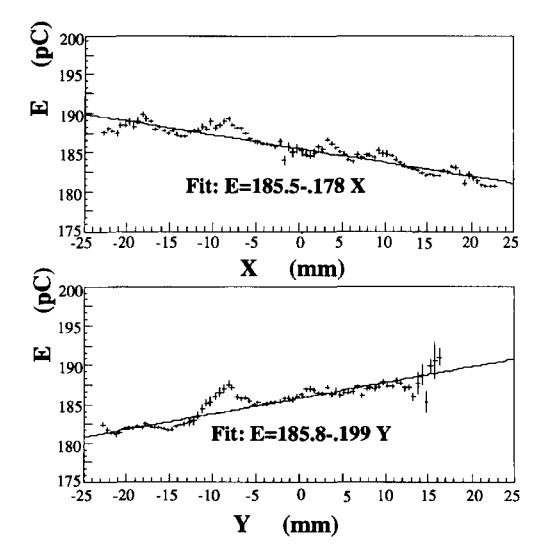
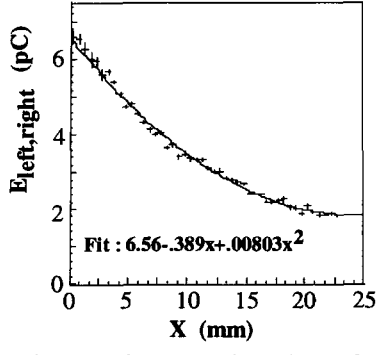


Fig. 12. X and Y beam profiles in tower 5 after leakage correction. The E = f(X) plot correspond to a  $|\Delta Y| = \pm 5$  mm slice and the E = f(Y) plot has been obtained for data in  $|\Delta X| = \pm 5$  mm slice around the center of tower 5. Data hitting the fibres regions are excluded (see section 4.5).

optical reflection constant of the small scintillator edges. In fact no special care was taken for these prototypes to achieve the same reflection power on the four lateral sides of the tower. This variation was fitted with a straight line as shown in Fig. 12. This last correction will be used in addition to the leakage correction for the final analysis of the data.

Fig. 13 shows the corrected spectrum of the total energy deposited by all the 40 GeV electrons data from Fig. 6 except the one which hit the tower edges and the fibre regions as defined in section 5. One sees that the resolution has been improved by more than 60%. A more detailed discussion of the resolution as function of the position of the impact point in tower 5 will be given in the next section.



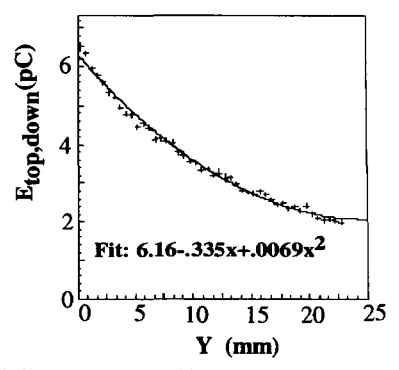


Fig. 11. Leakage correction estimated from 40 GeV electron data hitting the calorimeter.

# 5. Study of the calorimeter uniformity response

The data reported here have been taken with normal beam incidence to the tower what, as shown, induce non-uniformities in the calorimeter response. We have indicate a possible way to reduce these effects. So to give results free of systematic in what follows, the tower size will be limited to  $\Delta X = \pm 23$  mm and  $\Delta Y = \pm 23$  mm, so excluding the tower edges. We will also reject electrons hitting the fibre regions within a circle of radius equal to 1 mm centered at the fibre position.

For all the electron data taken in tower 5 (Fig. 6), we have displayed in Fig. 14 the deviation of the reconstructed energy to the overall mean energy as function of the X and Y electron impact coordinate. One sees that for the raw data the overall dispersion is of about  $\pm 3\%$ . When one compares the energy response at the center of the tower to the one measured at the edges, this last is lower by 3-4%. This is partly due to the noncontainment of the shower when one goes nearer to the tower limits. In addition Fig. 14a shows that at the left edge of tower 5 the energy is as high as at the center. One possible explanation for this

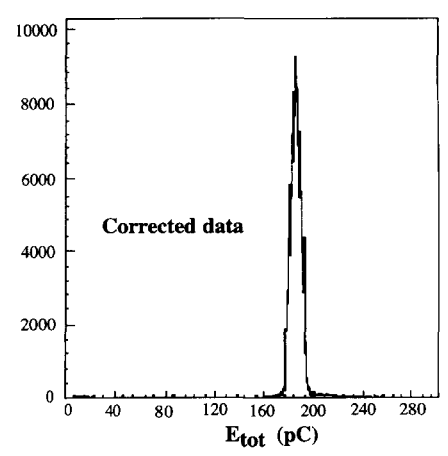


Fig. 13. Distribution of the corrected energy for 40 GeV electrons hitting tower 5. A Gaussian fit gives  $E_{\rm mean} = 186$  pC and  $\sigma/E = 2.05\%$ .

effect could be a higher reflection constant at this edge compared to ones of the other tower edges.

When one applies the energy corrections defined in the

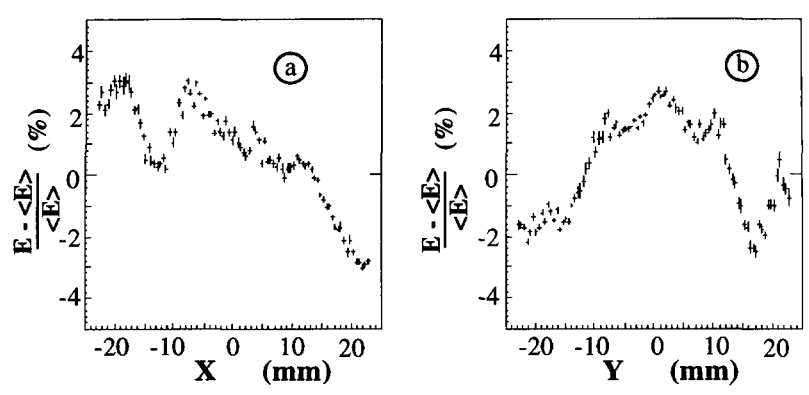


Fig. 14. Uniformity response for 40 GeV electron (raw data) hitting tower 5. (a) (and (b)) shows the energy deviations as function of X (and Y) impact point coordinates.

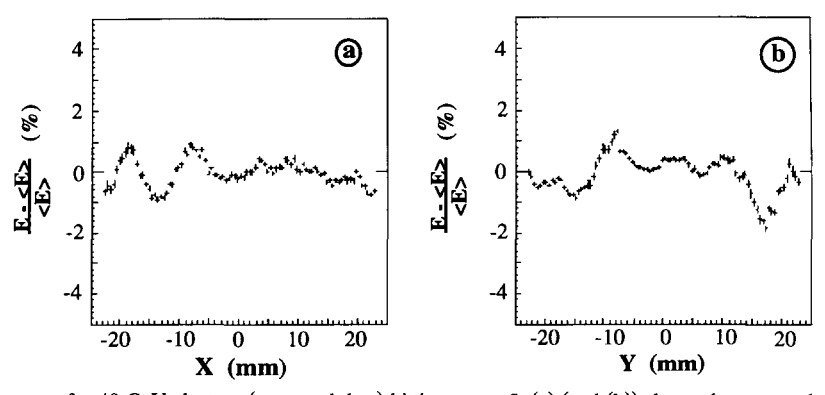


Fig. 15. Uniformity response for 40 GeV electron (corrected data) hitting tower 5; (a) (and (b)) shows the energy deviations as function of X (and Y) impact point coordinates. The corrections are described in the text.

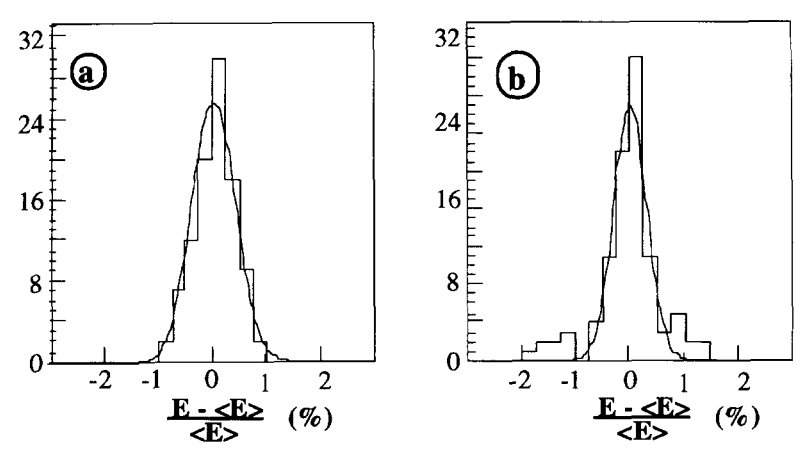


Fig. 16. Mean energy deviation for all 40 GeV electron data hitting tower 5. (a) Projection of Fig. 15a; (b) projection of Fig. 15b. Gaussian fits give a mean deviation of 0.05% for both projections. The fitted RMS are respectively  $\sigma = 0.4\%$  for (a) and  $\sigma = 0.3\%$  for (b).

previous section to the data, one obtains a uniformity response of better than  $\pm 1\%$  as it is shown in Fig. 15. Fig. 16 shows the projections of Figs. 15a and 15b on their

vertical axis. The curves are Gaussian fits to the data. The energy dispersions have respectively a  $\sigma = 0.4\%$  and 0.3% for X and Y beam profiles.

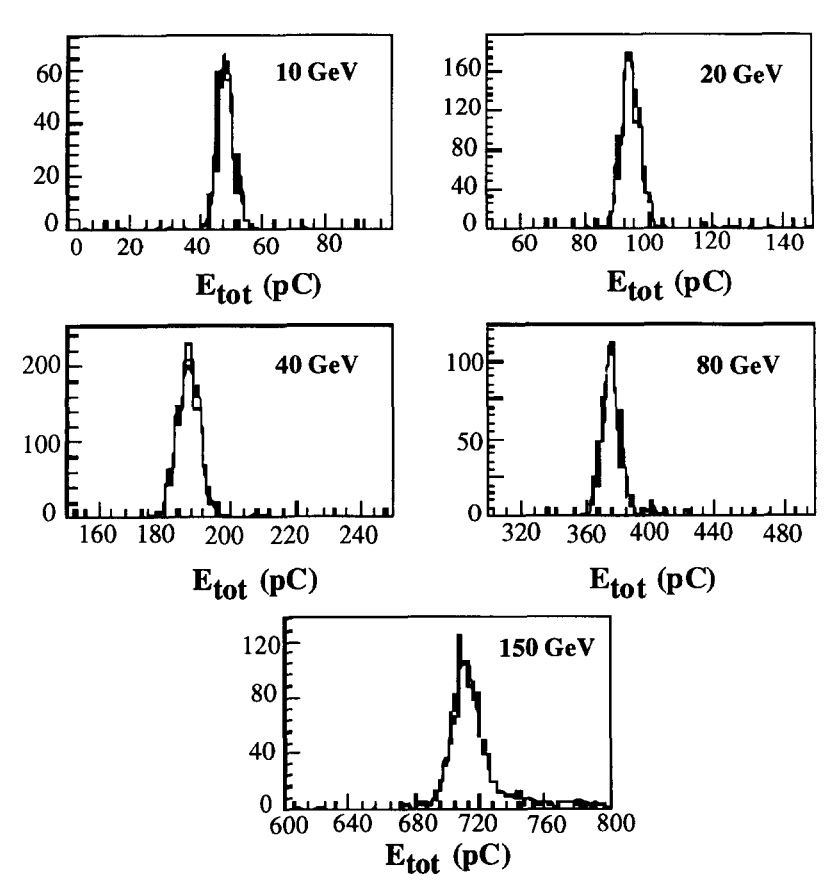


Fig. 17. Electron energy spectra measured with the Shashlik calorimeter.

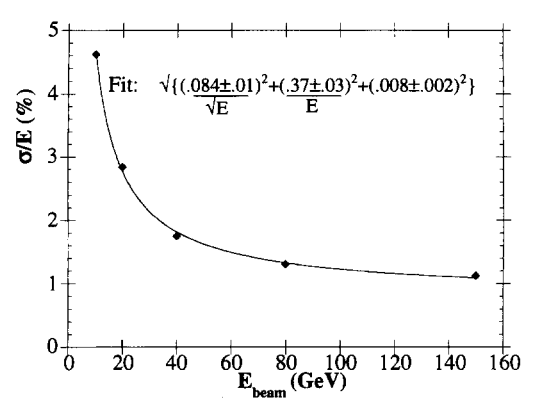


Fig. 18. Shashlik calorimeter energy resolution measurement.

The non-uniformity of the response of tower 5, under the conditions described in section 4.5, is after leakage and reflection coefficient differences corrections, at maximum  $\pm 1\%$ . The  $\sigma$  of the dispersions is much smaller (0.4%).

## 6. Energy resolution of the Shashlik calorimeter

To study the energy resolution, we have taken electron data at 10, 20, 40, 80 and 150 GeV with Trigger 2 conditions at the center of tower 5. The size of the beam spot was  $4 \times 4$  mm<sup>2</sup>. Fig. 17 shows the energy spectra for the five studied electron momenta. For 150 GeV electrons, a high energy tail is apparent. It is due to the shower tail not contained in the calorimeter and hitting the photodiode. Fig. 18 gives the variation of  $\sigma/E$  as function of the beam momentum. We have fitted the measured points to:

$$\frac{\sigma}{E} = \frac{a}{\sqrt{E}} \oplus \frac{b}{E} \oplus c,$$

where a represents the contribution of the sampling fluctuation, b the electronic noise term, and c the constant term contribution to the energy resolution.

The result of the fit is given in Table 2. This table also contains the results obtained for different types of readout which were used to read out the same towers. The sampling term achieved with a Si photodiode readout is 8.4%.

Table 2
Shashlik energy resolutions for various used readout systems

Readout	Best fit
PM	$\frac{\sigma}{E}(\%) = \frac{(9.0 \pm 0.1)}{\sqrt{E}} \oplus (1.0 \pm 0.3)$
PM+1 Si photodiode on tower 5 (central)	$\frac{\sigma}{E}(\%) = \frac{(8.4 \pm 0.6)}{\sqrt{E}} \oplus \frac{(0.084 \pm 0.006)}{E} \oplus (0.9 \pm 0.1)$
Si photodiodes	$\frac{\sigma}{E}(\%) = \frac{(8.4 \pm 0.1)}{\sqrt{E}} \oplus \frac{(0.37 \pm 0.03)}{E} \oplus (0.8 \pm 0.2)$

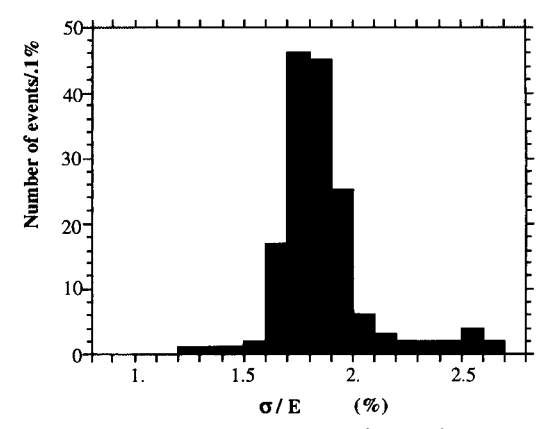


Fig. 19. Variation of  $\sigma/E$  for different  $(\Delta x, \Delta y) = 3 \times 3 \text{ mm}^2$  areas subdividing tower 5. 40 GeV electrons have been used for this study. A gaussian fit gives  $(\sigma/E)_{\text{mean}} = 1.86\%$  and  $\sigma = 0.06\%$ 

The constant term which comes out of the fits is always smaller than 1%. The electronic noise term, for a single diode readout when the Si photodiode was mounted on the central tower of the nonet, was measured to be  $84 \pm 6$  MeV. The electronic noise contribution to the energy resolution when the energy is obtained from the nine towers all read out with Si photodiodes is  $370 \pm 30$  MeV.

# 7. Effect of non-uniformity of tower response on the energy resolution

The 40 GeV electron data taken in tower 5 (Fig. 6) are here subdivided into subsamples covering  $(\Delta X, \Delta Y) = (3 \times 3) \text{ mm}^2$  areas. For each of these subsamples, we have performed on the energy spectrum a Gaussian fit giving us the mean energy and the energy dispersion. Fig. 19 gives the distribution of  $\sigma/E$  for all these subsamples. Apart of a small tail, all the measured values have a small dispersion. Fig. 20 shows the distributions of the dispersion of the fitted mean energies in each of the scanned boxes. As foreseen most of the data have a dispersion smaller than  $\pm 1\%$ . The RMS of this distribution is 0.7%.

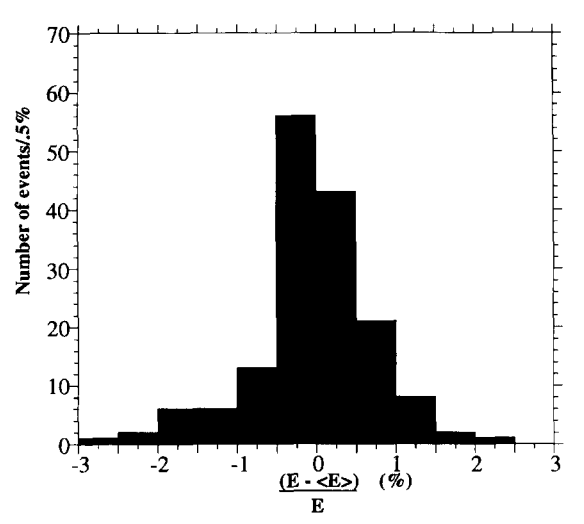


Fig. 20. Variation of energy dispersion for boxes of  $(\Delta x, \Delta y) = 3 \times 3 \text{ mm}^2$  areas subdividing tower 5. 40 GeV electrons have been used for this study. A Gaussian fit gives for the mean dispersion 0.008% and a  $\sigma = 0.7\%$ .

Assuming that the calorimeter has the resolution given in the previous section, we have recalculated the constant term for each of the subsamples. Fig. 21 gives the variation of the constant term for all the subsamples. For most of the data the constant term is smaller than 1%.

## 8. Shower position measurement

The shower center is provided by the mean of the transversal energy distribution accessed by using the following asymmetry variable:

$$A(x) = \frac{\sum_{i < i_{\text{max}}} E_i - \sum_{i > i_{\text{max}}} E_i}{E_{\text{tot}}},$$

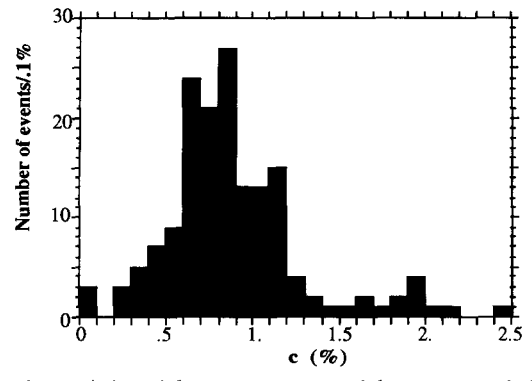


Fig. 21. Variation of the constant term c of the energy resolution for the  $(\Delta x, \Delta y) = 3 \times 3 \text{ mm}^2$  areas subsamples of tower 5. 40 GeV electrons have been used for this study. To estimate c we used the energy resolution obtained in section 6 i.e.  $\sigma / E(\%) = (8.4 \pm 0.1) / \sqrt{E} \oplus (0.37 \pm 0.03 / E \oplus (c))$ .

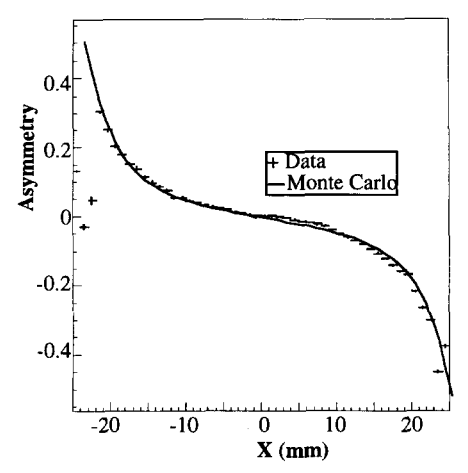


Fig. 22. Measured asymmetry for all 40 GeV electron data hitting tower 5. The curve shows the Monte Carlo prediction.

where  $i_{\rm max}$  denotes the interval in which the deposited energy is maximum. The details of this study are described elsewhere [15]. Fig. 22 shows the variation of the asymmetry as function of the electron impact in tower 5. The curve on the figure gives our Monte Carlo prediction. It well reproduces the data. The precision of the shower center is deduced from the asymmetry measurement using:

$$\delta x = \frac{1}{|dA/dx|} \sigma_{A}.$$

For our 40 GeV electron data we show in Fig. 23 the variation of the error on the shower position as a function of the electron impact point in the tower. It is clear that the precision is the worst at the center of the tower ( $\sigma_{x, y} = 1.8$  mm) and slowly improves when one approaches the tower edges ( $\sigma_{x, y} = 0.6$  mm).

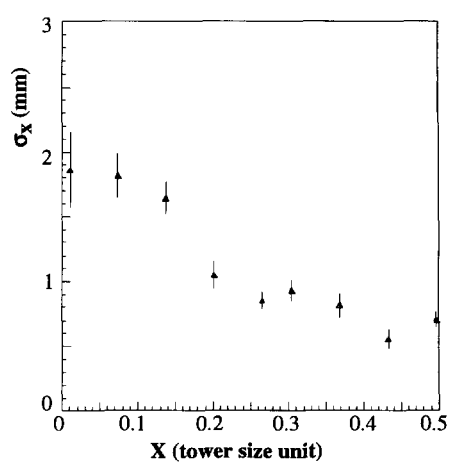


Fig. 23. Precision of the reconstructed shower position for 40 GeV electrons hitting tower 5.

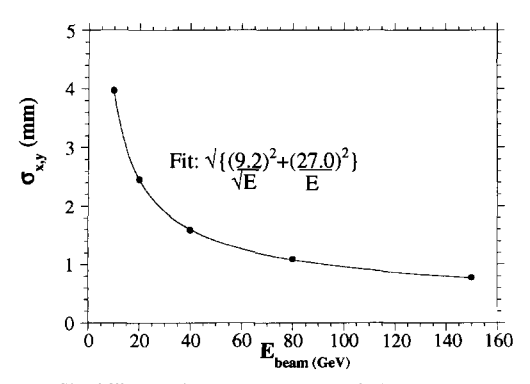


Fig. 24. Shashlik calorimeter position resolution. The curve is a best fit to the data.

The precision on the shower position has been measured at the tower center as function of the energy and is displayed in Fig. 24. The best fit to the data is obtained with a quadratic form of type:

$$\sigma_{x,y} = \frac{a}{\sqrt{E}} \oplus \frac{b}{E}$$

with

$$a = 9.2 \pm 0.3_{\text{stat}} \pm 0.7_{\text{syst}}$$
 (mm),

$$b = 27 \pm 1.4_{\rm stat} \pm 2.1_{\rm syst}$$
 (mm).

The curve on Fig. 24 well describes the data.

#### 9. Shower direction measurement

To achieve the measurement of the direction of a shower, one needs to have two independent position measurements. We assume that one position is given by the shower barycenter in the Shashlik and a second one by a preshower detector placed at about  $3X_0$ . To estimate the resolution on the shower direction, we have exposed the Shashlik calorimeter to electrons with  $4.5X_0$  lead in front of it. Fig. 25 gives the shower barycenter resolution for data with and without lead in front of the calorimeter. One sees that for 40 GeV electrons, we lose about 10% resolution on the tower center position measurement when  $4.5X_0$  lead is placed in front of the tower.

The variation of  $\sigma_{\theta}$  as function of the electron incident energy is given in Fig. 26. This prediction was obtained by using a infinite precise position prediction given by a preshower detector placed at about  $3X_0$  in front of the tower and the shower position obtained from the energy deposited in the calorimeter and extrapolated from measurements shown in Fig. 25. For this estimation we used as average longitudinal shower position  $\langle m \rangle$  (in  $X_0$  units) = 6.0 + 1.0 Ln E.

One sees that with a preshower detector associated to a

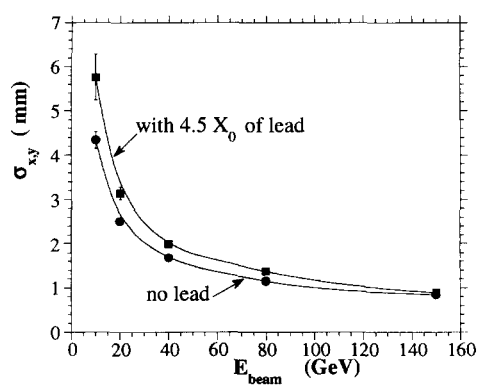


Fig. 25. Shashlik calorimeter shower position resolution with  $4.5X_0$  lead in front. For comparison results without lead are also given.

Shashlik calorimeter one could expect to achieve at the tower center an angular resolution of:

$$\sigma_{\theta}(\text{mrad}) = 70/\sqrt{E}$$
.

From Fig. 23, one can predicts that this resolution will improve by a factor of 3 when one goes near the tower edges. The mean expected angular resolution can be as good as:  $\sigma_{\theta}(mrad) = (40-50)/\sqrt{E}$ .

#### 10. Light yield of a Shashlik tower

The light yield provided by a Shashlik tower was measured with a Si photodiode supplied by a low-noise charge-sensitive amplifier. The gain of the amplifier was measured with a test charge injected through a calibration capacitance ( $C=1.6~\rm pF$ ) to the amplifier input. Our estimation of the systematic error in these measurements is  $\pm\,10\%$ .

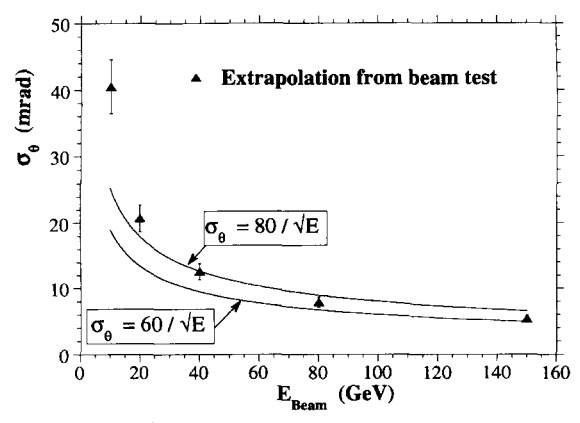


Fig. 26. Extrapolated angular resolution of the reconstructed shower direction when a preshower detector is placed in front of the Shashlik calorimeter.

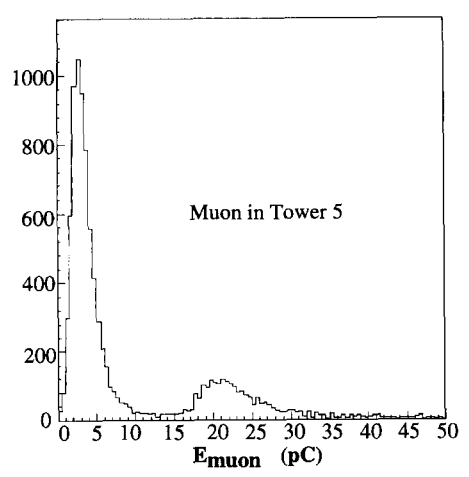


Fig. 27. Response to muons of a Shashlik calorimeter read out by Si photodiodes.

The light yield was measured in different experimental conditions. At first tower 5 of our setup was equipped with 13 K-27 fibers. The light yield provided by 40 GeV electron shower hitting the center of the tower gives in the photodiode a signal equal to 7300 electrons/GeV. As energy of the shower deposited in the tower represents 86% of the total energy of the shower and using the quantum efficiency (65%) of the Hamamatsu photodiode in the region of K-27 emission spectrum ( $\lambda = 525$  mm), one estimates that the total observed light yield is equal to 13 photons/MeV.

In a second test period, the towers were equipped with 25 Kuraray Y-7 WLS fibres. The light yield measurements were performed this time on seven towers. The photodiode efficiency for Y-7 ( $\lambda = 500$  nm) emission spectrum is 62.5%. For tower 5 we obtained this time 6400 electrons/ GeV to be compared with 7300 obtained for K-27 fibres. A mean value of 6600 electrons/GeV was measured for seven towers what corresponds to 12.3 photons/MeV for the Shashlik towers.

#### 11. Response to muons

Tower 5 of our calorimeter setup has been exposed to 225 GeV muons. Fig. 27 gives the measured energy spectrum. The estimated RMS noise for a single tower hit by muons being of the order of 100 MeV (0.5 pC) the muon peak is then clearly separated from the pedestal. The second peak located at 20 pC (about 4 GeV) comes from the muons hitting the Si photodiode. This last effect will be strongly reduced by the high magnetic field of the CMS detector (4 T) in which the Shashlik calorimeter will be placed. This is due to the fact that the photodiode is located at about 6-7 cm from the end of the tower consequence of the fibre bundle.

#### 12. Conclusions

The results presented here are the first obtained with a Shashlik calorimeter exposed to a high energy electron beams and read out with Si photodiodes.

The measured energy resolution is:

$$\frac{\sigma}{E}(\%) = \frac{(8.4 \pm 0.1)}{\sqrt{E}} \oplus \frac{(0.37 \pm 0.03)}{E} \oplus (0.8 \pm 0.2)$$

with E in GeV.

The shower position resolution was fitted to:

$$\sigma_{x,y}(\text{mm}) = \frac{9.2 \pm 0.3_{\text{stat}} \pm 0.7_{\text{syst}}}{\sqrt{E}}$$
$$\oplus \frac{27 \pm 1.4_{\text{stat}} \pm 2.1_{\text{syst}}}{E}.$$

The angular resolution of the direction of an electron shower was estimated with using one point from a preshower detector located at  $3X_0$  and the second point on a barycenter in the calorimeter mosaic. The result is encouraging being in agreement with a mean resolution of:

$$\sigma_{\theta}(\text{mrad}) = 50/\sqrt{E}$$
.

that gives for an electron of 50 GeV an angular resolution of 7 mrad.

Finally an extensive study of the uniformity of the response of the calorimeter is presented in this work. It is shown that  $\pm 1\%$  uniformity could be easily achieved. The effect of the non-uniformity on the constant term of the energy resolution is small.

# Acknowledgements

The work described in this paper would have been impossible without the outstanding technical support provided by our engineers and technicians. The data presented here were taken with the RD1 beam setup and DAQ; we are grateful to our colleagues from RD1 collaboration and in particular J.M. Gaillard, L. Linssen and L. Poggioli who made our running condition possible and easy. And finally, we are grateful to the staff of the SPS for the excellent beam conditions and assistance provided during out tests.

#### References

- [1] LHC Workshop, CERN 90-10, Aachen, 4-9 Oct. 1990.
- [2] C. Seez and T.S. Virdee, Imperial College Preprint IC/HEP 92/4 (1992).
- [3] H. Fessler et al., Nucl. Instr. and Meth. 228 (1985) 303.
- [4] G.S. Atoyan et al., Nucl. Instr. and Meth. A 320 (1992) 144, Preprint INR-736/91, INR, Moscow (1991).
- [5] B. Loehr et al., Nucl. Instr. and Meth. A 254 (1987) 26.
- [6] D. Autiero, HEP Marseille Conf., July 22-28, 1993.

- [7] CMS The Compact Muon Solenoid, Letter of Intent CERN/ LHCC 92-3, LHCC/I1 (1992).
- [8] J. Badier et al., CMS TN/92-45 and X-LPNHE/93-2.
- [9] V.K. Semenov et al., Preprint JINR 13-90-16, Dubna (1990) in Russian.
- [10] J. Badier et al., Preprint CMS TN/93-66, INR 821/93, X-LPNHE/93-4.
- [11] Labarga and E. Ros, Preprint University of Siegen, FTUA EP-86-3 (1986).
- [12] The aluminization was done by Precitrame S.A., CH-2 Tramelan, Switzerland.
- [13]  $10 \times 10 \text{ mm}^2$  Hamamatsu S3590-05 photodiodes.
- [14] LeCroy 2282 ADC (1000 pC) with 0.25 pC/channel.
- [15] Badier et al., CMS TN/ 93-65.